BG 35a

Met.O.835

METEOROLOGICAL OFFICE

Scientific Paper No. 31

The Three-dimensional Analysis of Meteorological Data

by R. DIXON, B.Sc. and E. A. SPACKMAN, M.Sc.

METEOROLOGICAL OFFICE
13524
-4 FEB 1971
H. Q. ST. C.
R.A.F. HIGH WYCOMBE

LONDON: HER MAJESTY'S STATIONERY OFFICE

PRICE 7s 6d (37½p) NET

Met.O.835

METEOROLOGICAL OFFICE

Scientific Paper No. 31

The Three-dimensional Analysis of Meteorological Data

by R. DIXON, B.Sc. and E. A. SPACKMAN, M.Sc.

LONDON
HER MAJESTY'S STATIONERY OFFICE
1970

U.D.C. 551.501.42:
551.509.313:
521.3:
681.31/34

Contents

Summary 1
Introduction 1
Theory 1
The experiment 6
The 1000-mb evaluations 8
The 850-mb evaluations 11
The 700-mb evaluations 14
The 500-mb evaluations 17
The 200-mb evaluations 20
The 100-mb evaluations 23
The MSL pressure chart 25
Comments 27
Acknowledgement 28
Bibliography 28

The Three-dimensional Analysis of Meteorological Data

by R. Dixon, B.Sc. and E. A. Spackman, M.Sc.

SUMMARY

There is a need for meteorological observations to be rigorously analysed in three dimensions to meet the initial data requirements of modern atmospheric models used in numerical forecasting. This paper presents a method in which a high-power trivariate polynomial is fitted to the data within a large volume of the atmosphere. Some preliminary results are presented. The work described is an extension of that reported in *Scientific Paper* No. 30.

INTRODUCTION

Dixon[1]* has described the theoretical basis of data analysis using orthogonal polynomials and has presented evidence on the application of this technique to the two-dimensional analysis of height and wind data at standard pressure levels. He also indicated the theoretical extension of the method to the three- or four-dimensional problem. The present paper gives further theoretical details for the three-dimensional case, and presents the results of a preliminary experiment which may help in assessing the feasibility and desirability of this type of analysis. The main purpose of this approach is to develop an automatic analysis system capable of obtaining full value from the large amount of data for non-standard levels and times which will become available in the near future. It is considered that this can be achieved by building the analysis system around a data-fitting technique which has an intrinsic four-dimensional capability. In due course, when adequate computing facilities are available, it is hoped to carry out similar experiments using four-dimensional data. In the meantime three-dimensional exercises provide useful experience in applying the method.

THEORY

In the two-dimensional work orthonormalized polynomials corresponding to the base functions

$$1,\ x,\ y,\ x^2,\ xy,\ y^2,\ x^3,\ x^2y,\ xy^2,\ y^3,\ x^4,\ \ldots\ , \qquad \ldots\ (1)$$

were generated in the sequence

$$\begin{array}{lllll} \phi_0(1) & & & & \\ \phi_1(x) & \phi_2(y) & & & \\ \phi_3(x^2) & \phi_4(xy) & \phi_5(y^2) & & \\ \phi_6(x^3) & \phi_7(x^2y) & \phi_8(xy^2) & \phi_9(y^3) & \\ \phi_{10}(x^4) & \phi_{11}(x^3y) & \phi_{12}(x^2y^2) & \phi_{13}(xy^3) & \phi_{14}(y^4) \\ \cdots\cdots & \cdots\cdots & \cdots\cdots & \cdots\cdots & \cdots\cdots \end{array} \qquad \ldots\ (2)$$

and so on, where $\phi_7(x^2y)$ means a polynomial in the space variables x and y having all terms in the sequence (1) up to and including x^2y but not beyond. The first three ϕs were generated by the Gram-Schmidt process and the remainder by the use of the two recurrence relationships

* The superscript figures refer to the bibliography on page 28.

$$\phi_j = x\phi_{j-i} - \sum_{l=j-2i+1}^{l=j-1} c_l\phi_l \quad \ldots (3)$$

where $c_l = \phi_l \cdot \mathbf{x}\phi_{j-i}$ for ϕs in the body of the triangular scheme (2), and

$$\phi_j = y\phi_{j-i-1} - \sum_{l=j-2i-1}^{l=j-1} c_l\phi_l \quad \ldots (4)$$

where $c_l = \phi_l \cdot \mathbf{y}\phi_{j-i-1}$ for ϕs on the hypotenuse. In (3) and (4) j is the number of the ϕ and i is the degree.

In the three-dimensional experiment orthonormalized polynomials corresponding to the base functions

$$1, x, y, p, x^2, yx, y^2, px, py, p^2, x^3, yx^2, \ldots, \quad \ldots (5)$$

were generated in the sequence

$$\left.\begin{array}{l} \phi_0(1) \\ \phi_1(x) \quad \phi_2(y) \quad \phi_3(p) \\ \phi_4(x^2) \quad \phi_5(yx) \quad \phi_6(y^2) \quad \phi_7(px) \quad \phi_8(py) \quad \phi_9(p^2) \\ \phi_{10}(x^3), \ldots, \end{array}\right\} \quad \ldots (6)$$

and so on, where p represents log (pressure). This time the whole sequence of orthonormal polynomials was generated by the Gram-Schmidt process

$$\phi_0 = \mathbf{1} \quad \ldots (7a)$$

$$\phi_1 = \mathbf{x} - (\phi_0 \cdot \mathbf{x})\phi_0 \quad \ldots (7b)$$

$$\phi_2 = \mathbf{y} - (\phi_0 \cdot \mathbf{y})\phi_0 - (\phi_1 \cdot \mathbf{y})\phi_1 \quad \ldots (7c)$$

$$\phi_3 = \mathbf{p} - (\phi_0 \cdot \mathbf{p})\phi_0 - (\phi_1 \cdot \mathbf{p})\phi_1 - (\phi_2 \cdot \mathbf{p})\phi_2 \quad \ldots (7d)$$

$$\phi_4 = \mathbf{x}^2 - (\phi_0 \cdot \mathbf{x}^2)\phi_0 - , \ldots, \quad \ldots (7e)$$

each ϕ being normalized immediately after formation by dividing by $\sqrt{(\phi_r \cdot \phi_r)}$.

However, if a long string of ϕs is generated by a straight application of (7) there is some danger that the problem of ill-conditioning will arise again, the reason being that the steady accumulation of round-off error results in the later ϕs not being strictly orthogonal. In fact it is known that once appreciable contamination of the orthogonal vectors by round-off error has occurred the process quickly collapses.[2] This tendency was suppressed by forming each vector in stages, not directly as in (7). For example, ϕ_1 having been generated, ϕ_2 was then formed by the sequence

$$\left.\begin{array}{l} \phi_2^0 = \mathbf{y} - (\mathbf{y} \cdot \phi_0)\phi_0 \\ \quad \text{normalize} \\ \phi_2^1 = \phi_2^0 - (\phi_2^0 \cdot \phi_1)\phi_1 \\ \quad \text{normalize} \end{array}\right\} \quad \ldots (8)$$

and similarly for the other ϕs.

To see why this scheme has the desired effect, consider the part played by the term

$(\phi_1 \cdot \mathbf{y})\phi_1$ in (7*c*). It represents the removal from the vector $\mathbf{y}$ of the component of $\mathbf{y}$ in the direction of ϕ_1, thus ensuring that ϕ_2 will be orthogonal to ϕ_1. Now suppose that when ϕ_1 was computed at the previous stage it was not truly orthogonal to ϕ_0, but contained an error $\varepsilon\phi_0$, so that

$$ {}^{E}\phi_1 = \phi_1 + \varepsilon\phi_0 \qquad \ldots (9) $$

where ${}^{E}\phi_1$ denotes the contaminated vector. If ϕ_2 is formed directly, using (7*c*), a contaminated ϕ_2, denoted by ${}^{E}\phi_2$ will result. In fact,

$$ \begin{aligned} {}^{E}\phi_2 &= \mathbf{y} - (\phi_0 \cdot \mathbf{y})\phi_0 - ({}^{E}\phi_1 \cdot \mathbf{y}){}^{E}\phi_1 \\ &= \mathbf{y} - (\phi_0 \cdot \mathbf{y})\phi_0 - [(\phi_1 + \varepsilon\phi_0) \cdot \mathbf{y}](\phi_1 + \varepsilon\phi_0) \\ &= \mathbf{y} - (\phi_0 \cdot \mathbf{y})\phi_0 - (\phi_1 \cdot \mathbf{y})\phi_1 - (\varepsilon\phi_0 \cdot \mathbf{y})\phi_1 - (\phi_1 \cdot \mathbf{y})\varepsilon\phi_0 - (\varepsilon\phi_0 \cdot \mathbf{y})\varepsilon\phi_0 \end{aligned} \qquad \ldots (10) $$

and it is seen by comparing the right-hand side of (10) with (7*c*) that the error in ${}^{E}\phi_1$ results in the subtraction of the wrong amount of ϕ_1. If, instead of (7*c*) the indirect sequence (8) is used, there results

$$ \begin{aligned} {}^{E}\phi_2^1 &= \phi_2^0 - (\phi_2^0 \cdot {}^{E}\phi_1){}^{E}\phi_1 \\ &= \mathbf{y} - (\mathbf{y} \cdot \phi_0)\phi_0 - \{[\mathbf{y} - (\mathbf{y} \cdot \phi_0)\phi_0] \cdot (\phi_1 + \varepsilon\phi_0)\}(\phi_1 + \varepsilon\phi_0) \\ &= \mathbf{y} - (\mathbf{y} \cdot \phi_0)\phi_0 - (\mathbf{y} \cdot \phi_1)\phi_1 - \{\varepsilon\phi_0 \cdot [\mathbf{y} - (\mathbf{y} \cdot \phi_0)\phi_0]\}(\phi_1 + \varepsilon\phi_0) - (\mathbf{y} \cdot \phi_1)\varepsilon\phi_0, \end{aligned} $$

but on the right-hand side the term $\{\varepsilon\phi_0 \cdot [\mathbf{y} - (\mathbf{y} \cdot \phi_0)\phi_0]\}(\phi_1 + \varepsilon\phi_0)$ is zero. This follows because the vector $[\mathbf{y} - (\mathbf{y} \cdot \phi_0)\phi_0]$ is orthogonal to $\varepsilon\phi_0$ and the scalar product is therefore zero. So finally

$$ {}^{E}\phi_2^1 = \mathbf{y} - (\mathbf{y} \cdot \phi_0)\phi_0 - (\mathbf{y} \cdot \phi_1)\phi_1 - (\mathbf{y} \cdot \phi_1)\varepsilon\phi_0 \qquad \ldots (11) $$

and by contrast with (10) this time there is no ϕ_1 contamination. Thus application of the computational device (8) at all stages results in the removal of any contamination by the previous vector in the Gram-Schmidt sequence.

Opportunities for the use of this device occur fairly frequently in this type of work, and the principle involved should be well understood, as it can make the difference between sense and nonsense in any large-scale application. Variants of it have appeared in the literature,[2, 3] its earliest appearance being due to Cadwell and Williams.[4]

It is also worth noting that a Gram-Schmidt sequence can be generated in the form

$$ \left.\begin{aligned} \phi_0 &= \mathbf{1} \\ \phi_1 &= \mathbf{x} - \left[\frac{\phi_0 \cdot \mathrm{W} \cdot \mathbf{x}}{\phi_0 \cdot \mathrm{W} \cdot \phi_0}\right]\phi_0 \\ \phi_2 &= \mathbf{y} - \left[\frac{\phi_0 \cdot \mathrm{W} \cdot \mathbf{y}}{\phi_0 \cdot \mathrm{W} \cdot \phi_0}\right]\phi_0 - \left[\frac{\phi_1 \cdot \mathrm{W} \cdot \mathbf{y}}{\phi_1 \cdot \mathrm{W} \cdot \phi_1}\right]\phi_1 \\ \phi_3 &= \mathbf{p} - \left[\frac{\phi_0 \cdot \mathrm{W} \cdot \mathbf{p}}{\phi_0 \cdot \mathrm{W} \cdot \phi_0}\right]\phi_0 - \ldots, \end{aligned}\right\} \qquad \ldots (12) $$

normalizing at each stage by dividing by $\sqrt{(\phi_r \cdot \mathrm{W} \cdot \phi_r)}$ where W is any diagonal matrix.[5] In

practice the diagonal elements of W can be the weights assigned to each observation. The weights may be chosen on common-sense grounds as in the majority of current operational systems, or they may be determined as an optimal set, by a least-squares criterion on the statistical structure functions of the field, as is done in the Russian method of 'analysis by optimal interpolation',[6] though the structure functions might have to be a different set from those currently used. It may be remarked here that if the Russian method of optimal interpolation is to be extended to the three-dimensional or four-dimensional case then it will probably be necessary to make some orthogonalization routine available to it in order to overcome the ill-conditioning of the equations which determine the weights.[7] Thus the Russian principle of optimal interpolation and the method being presented should combine quite conveniently. The provision of the W-facility is quite important as it is via W that the 'meteorology' can be injected into what is an otherwise purely mathematical process. This is perhaps especially true if W is determined from the statistical structure of the field.

In any operational application of this method the scalar coefficients of the Gram-Schmidt sequences (7), (8) or (12) would be worth preserving, as estimates of various statistical parameters may be calculated directly in terms of them, thus avoiding further lengthy calculations. This possibility has already been noted.[5]

So far the theoretical description has been in terms of $N+1$-vectors in an observation space of $N+1$ dimensions, using the simple sequence of Cartesian base functions (1). For many practical purposes this will suffice and is the most convenient scheme, but the method is not confined to $N+1$-vectors, and any set of initial base functions can be used in place of (1). If the field of observations being fitted is a physical space vector such as wind velocity instead of a scalar such as pressure height, then two sets of initial base functions may be chosen, one for each component of the physical vector, in such a way as to impose some condition on the physical vector field. To illustrate this, let $N+1$ observations of a two-dimensional physical vector $\mathbf{V}(u,v)$ be given, so that there are observation-space vectors

$$\left.\begin{aligned} \mathbf{u} &\equiv \mathbf{u}(u_0, u_1, u_2, \ldots, u_N) \\ \mathbf{v} &\equiv \mathbf{v}(v_0, v_1, v_2, \ldots, v_N). \end{aligned}\right\} \quad \ldots (13)$$

The fitting can be done in terms of two sets of base functions f_r and g_r, $r=0, 1, 2, \ldots, n$, so that

$$\left.\begin{aligned} \mathbf{u} &= a_0\mathbf{f}_0 + a_1\mathbf{f}_1 + a_2\mathbf{f}_2 + \ldots + a_n\mathbf{f}_n + \mathbf{R}_n \\ \mathbf{v} &= a_0\mathbf{g}_0 + a_1\mathbf{g}_1 + a_2\mathbf{g}_2 + \ldots + a_n\mathbf{g}_n + \mathbf{S}_n \end{aligned}\right\} \quad \ldots (14)$$

where $\mathbf{R}_n$ and $\mathbf{S}_n$ are vectors of residuals.

To do this vectors of dimensionality $2N+2$ are introduced so that

$$\left.\begin{aligned} \mathbf{V} &\equiv \mathbf{V}(u_0, u_1, u_2, \ldots, u_N, v_0, v_1, v_2, \ldots, v_N) \\ \mathbf{l}_r &\equiv \mathbf{l}_r(f_{r0}, f_{r1}, f_{r2}, \ldots, f_{rN}, g_{r0}, g_{r1}, g_{r2}, \ldots, g_{rN}) \\ \mathbf{E}_n &\equiv \mathbf{E}_n(R_{n0}, R_{n1}, R_{n2}, \ldots, R_{nN}, S_{n0}, S_{n1}, S_{n2}, \ldots, S_{nN}) \end{aligned}\right\} \quad \ldots (15)$$

and, for the least-squares fitting, the coefficients in

$$\mathbf{V} = a_0\mathbf{l}_0 + a_1\mathbf{l}_1 + a_2\mathbf{l}_2 + \ldots + a_n\mathbf{l}_n + \mathbf{E} \quad \ldots (16)$$

are determined to be the set which minimizes $\mathbf{E}_n \cdot \mathbf{E}_n$. This is accomplished as before by orthonormalizing the base vectors $\mathbf{l}_r$, using the Gram-Schmidt method, the important possibility here being that the base functions f_r and g_r can be selected, for example, so that

$$\frac{\partial f_r}{\partial x} + \frac{\partial g_r}{\partial y} = 0. \qquad \ldots (17)$$

In this case, the observations of $\mathbf{V}(u, v)$ are fitted according to the least-squares principle, but subject to the global condition that div $\mathbf{V} \equiv 0$.

It will be appreciated that orthonormalization of the $\mathbf{l}_r$ will not upset the condition div $\mathbf{V} \equiv 0$ since the Gram-Schmidt process involves only the formation of linear combinations of previous vectors at each stage. This possibility is clearly implicit in the algebra of least squares using orthogonalization processes, and was utilized by Fougere[8] to fit magnetic-field data for the earth in such a way that the radial component of the curl of the magnetic field was zero.

The orthonormal $\boldsymbol{\phi}$ vectors having been generated, the coefficients of the fitting expression

$$\mathbf{z} = a_0\boldsymbol{\phi}_0 + a_1\boldsymbol{\phi}_1 + a_2\boldsymbol{\phi}_2 + a_3\boldsymbol{\phi}_3 + a_4\boldsymbol{\phi}_4 + \ldots, \qquad \ldots (18)$$

where $\mathbf{z}$ is the vector of fitted height values, were obtained from

$$a_r = \mathbf{h} \cdot \boldsymbol{\phi}_r \qquad \ldots (19)$$

where $\mathbf{h}$ is the vector of observed height values. Corresponding to the vector expression (18) there is then

$$z = a_0\phi_0 + a_1\phi_1 + a_2\phi_2 + a_3\phi_3 + a_4\phi_4 + \ldots, \qquad \ldots (20)$$

in terms of the ϕ base functions themselves. Although the reordering is not essential it is convenient to reshuffle (20) into the form

$$z = b_0 + b_1x + b_2y + b_3p + b_4x^2 + b_5xy + \ldots, \qquad \ldots (21)$$

i.e.

$$z = \mathrm{f}(x, y, p) \qquad \ldots (22)$$

in which form it is easily evaluated for any values of the independent variables.

The evaluation of the coefficients a_n affords another opportunity for employing the decontamination technique. If the residual vectors at each stage are denoted by $\mathbf{r}_0, \mathbf{r}_1, \mathbf{r}_2, \ldots$, then

$$\left.\begin{aligned} \mathbf{r}_1 &= \mathbf{h} - a_0\boldsymbol{\phi}_0 \\ \mathbf{r}_2 &= \mathbf{r}_1 - a_1\boldsymbol{\phi}_1 \\ \mathbf{r}_3 &= \mathbf{r}_2 - a_2\boldsymbol{\phi}_2 \\ &\cdots \\ \mathbf{r}_{r+1} &= \mathbf{r}_r - a_r\boldsymbol{\phi}_r\,, \end{aligned}\right\} \qquad \ldots (23)$$

and

$$\mathbf{a}_r = \mathbf{r}_r \cdot \boldsymbol{\phi}_r. \qquad \ldots (24)$$

On analysis the use of (23) and (24) rather than (19) is found to be a simpler example of the principle behind the use of (8) in the Gram-Schmidt process.

Besides the evaluation of (22) to provide the usual type of height analysis for given pressure levels, it is readily seen that (22) will yield vertical cross-sections and various other types of field by differentiation. For example, it follows from the hydrostatic relationship that temperature fields are available upon differentiating with respect to p, whilst a second differentiation with respect to p yields lapse rates. Fields normally obtained by using finite differences, such as geostrophic isotachs, can be obtained by using true differentials, though of course finite-difference evaluations can still be made for those processes which are currently dependent upon finite-difference technology.

THE EXPERIMENT

For each of the seven adjacent regions shown in Figure 1 a sixth-power trivariate polynomial was fitted to data between the surface and 100-mb levels for 00 GMT on 14 November 1968 The data used were of three kinds:

(i) significant-level heights calculated from parts B and D of the upper air TEMP messages,

(ii) background heights taken from the 12-hour numerical forecasts for 1000 mb, 500 mb, 200 mb and 100 mb based on data at 12 GMT on 13 November 1968, and

(iii) heights manufactured from the significant-level wind reports by assuming the geostrophic relationship between wind and contour gradient. No corrections for curvature were made.

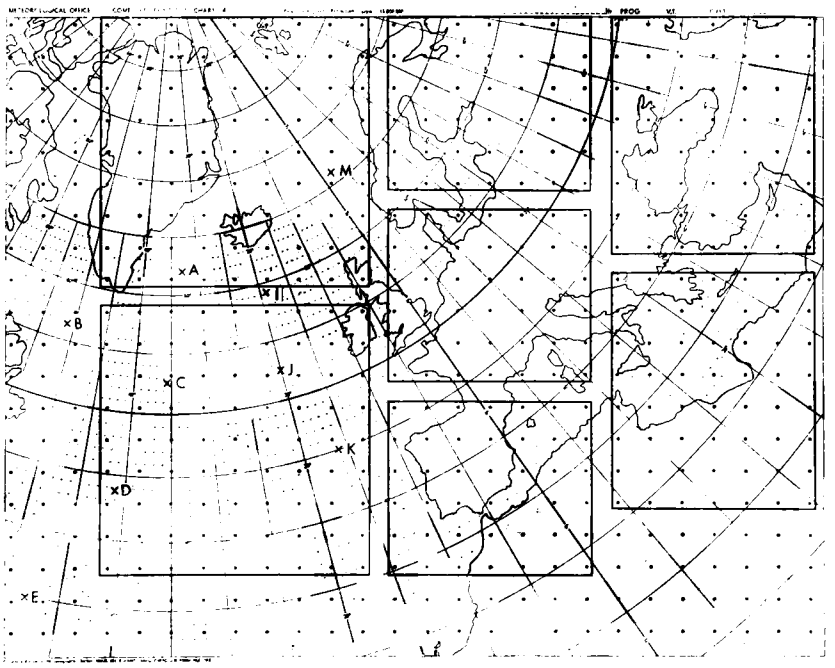

FIGURE 1. Chart showing the numerical grid points and the seven adjacent regions used in the experiment.

Experience with the fitting of two-dimensional fields has suggested that an eighth-power polynomial fitting would be more appropriate for this experiment than a sixth-power polynomial. However, computer limitations made it impracticable to attempt more than a sixth-power fitting and even to achieve this it was necessary to use half-length working. Use of a sixth power has meant that there is a considerable element of underfitting to be allowed for in considering the results. The limitations of the KDF 9 computer also imposed the following deficiencies in data handling:

(i) Not all significant-level height and wind data could be used. A selection was made depending upon the density of stations and the number of significant levels reported.
(ii) Background heights from the 12-hour numerical forecasts could not be used liberally. A routine was written which assessed the three-dimensional density of significant-level data available in the neighbourhood of a grid point at 1000, 500, 200 and 100 mb and inserted a background value if the density was below a certain criterion.
(iii) All data were used in their raw state. The systematic national radiosonde errors were not removed, neither were corrections made to observations having a large random error.
(iv) All data were given unit weight.

The sixth-power trivariate polynomials having been fitted for each of the seven volumes, grid-point fields of height, temperature and lapse rate, and geostrophic isotachs were obtained for 1000, 850, 700, 500, 300, 250, 200, 150 and 100 mb by an appropriate evaluation of the $z = f(x, y, p)$ functions, the relevant differentiations having been performed first in the case of temperature, lapse rate and isotachs. In addition, by using the 1000-mb height and the 1000-mb temperature field so obtained, a map of surface pressure was obtained by downward extrapolation. For each particular field the grid-point evaluations from each separate area were inserted in a master array and printed out as one field, using a zebra-contour printing routine. The only action taken to ensure merging at the edges of the separate areas was that an overlap of $1\frac{1}{2}$ grid lengths was allowed in the raw data. Thus within these limits some observations were used in more than one area, which guaranteed a measure of matching at the edges. Naturally this provision was not adequate to guarantee complete merging and in some of the fields produced, especially those depending on differentiation, the edges of the areas can be plainly seen, as was expected. (Figures 3–6, 8–11, 13–16, 18–21, 23–26 and 28–31. Contour heights indicated in geopotential decametres).

There are a number of processes which might have been applied to the evaluated grid-point values at the edges to give a better merging, but in a preliminary experiment of this nature it was thought better to allow the magnitude of the merging problem to be seen.

The case chosen for this experiment, that of 00 GMT on 14 November 1968, presented some difficulty for the current operational analysis routines, the situation around ocean weather station 'C' being very poorly analysed. The case was subjected to considerable study with respect to the operational techniques and for this reason the data were still available on magnetic tape at the time when this experiment was proposed.

The hand-drawn subjectively analysed charts produced by the Central Forecasting Office (CFO) are shown in Figures 2, 7, 12, 17, 22 and 27. Whilst these charts are the ones traditionally used for the purpose of assessing the results of an objective process, it must be remembered that they are also subject to error, and in fact a study of the original charts does show some inconsistencies.

Note: contour heights shown in the diagrams are in geopotential decametres, not gpm.

THE 1000-MB EVALUATIONS

Figure 3

The main features of the contour-height field were well fitted except for the low near the ship at ocean weather station 'A', which, although of the right depth, is on the wrong side of the ship. The reason for this is thought to be the lack of significant-level wind data at ocean weather station 'A' and Keflavik, plus the effect of a large random error, which at 100 mb was +15 geopotential decametres. It is worth noting that the edges of the separate areas, though discernible, do not stand out.

Figure 4

In the main the temperatures are of the right order, as far as can be judged from the CFO surface chart (Figure 2), except in the areas where data are really sparse. Over north Africa in particular the point is brought out that background values at four levels only are not sufficient in an area with an almost total lack of observations. As was expected, the edges of the separate areas show clearly. The 1000-mb level being the bottom face of the fitted volume the derivative of height is not well defined and this affects both the temperature values and the edge merging.

Figure 5

The effect of being on the face of the fitted volume is even more marked in this second-derivative field. The edges stand out very clearly, and the values are unrealistic over much of the chart, doing little more than confirm a decrease in stability from north to south.

Figure 6

This shows that the geostrophic isotach pattern is reasonably correct in its main features as far as can be judged against the CFO surface chart (no CFO 1000-mb chart is available).

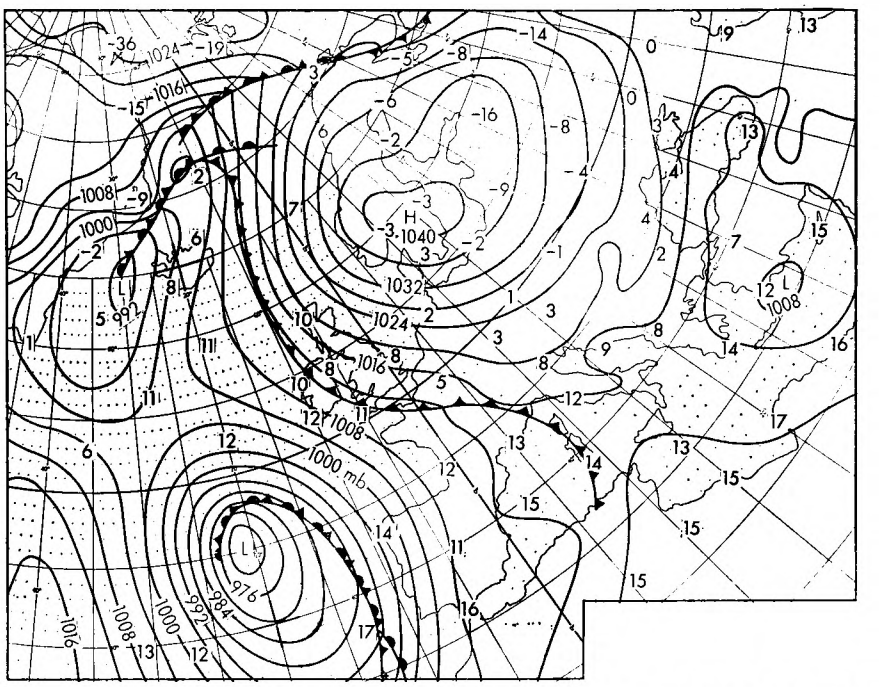

FIGURE 2. MSL surface pressure chart for 00 GMT, 14 November 1968, hand-drawn in the Central Forecasting Office. Isobars are at intervals of 4 mb. Temperatures in degrees Celsius are shown for selected locations.

FIGURE 3. Cross-section at 1000 mb of 6th-power trivariate polynomials. Contours are at intervals of 3 geopotential decametres.

FIGURE 4. Isotherms at 1000 mb obtained by differentiation of the 6th-power trivariate polynomials.
Isotherms are at intervals of 3 degC.

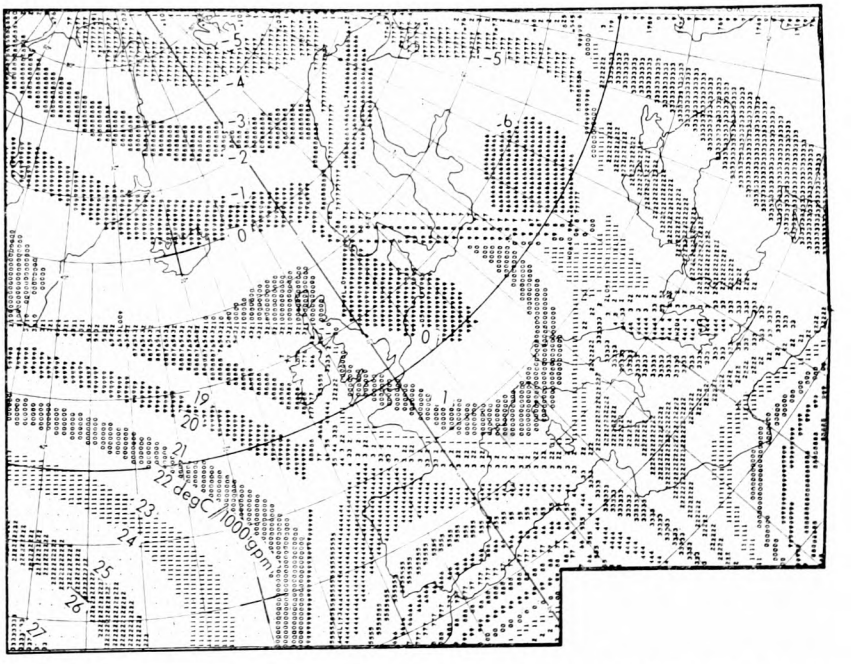

FIGURE 5. Isopleths of lapse rate at 1000 mb obtained by differentiation of the 6th-power trivariate polynomials.
Isopleths are at intervals of 1 degC/1000 gpm.

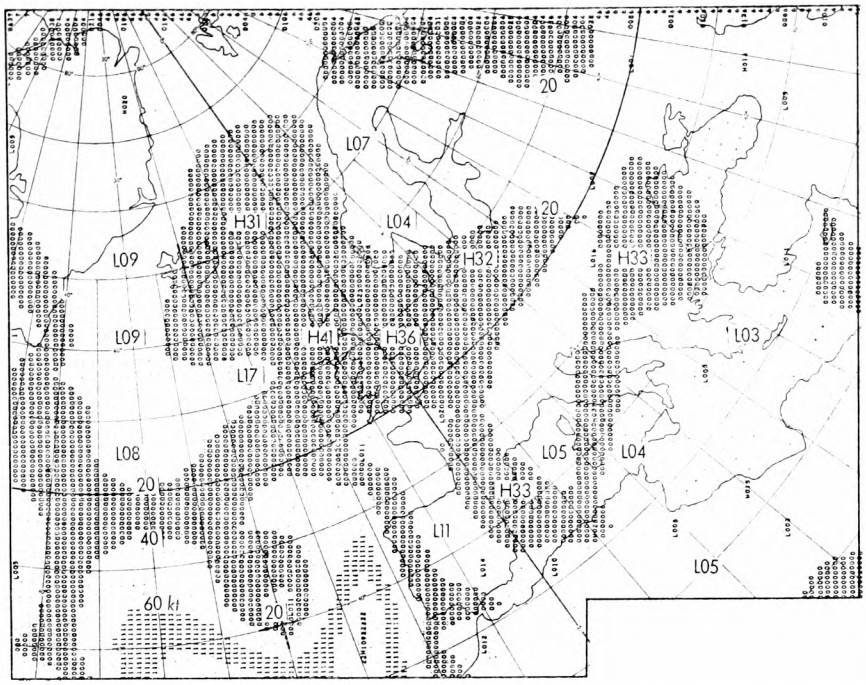

FIGURE 6. Geostrophic isotachs at 1000 mb obtained by differentiation of the 6th-power trivariate polynomials.
Isotachs are at intervals of 20 kt.

THE 850-MB EVALUATIONS

Figure 8

A direct comparison with a CFO chart (Figure 7) being possible for this level, it can be seen that the main features of the contour pattern are well placed, with fairly accurate central values.

Figure 9

By contrast with the 1000-mb level (Figure 4) the temperature field is now quite realistic and surprisingly accurate over much of the chart, even the north African area having reasonable values. Although the edges can be seen the discrepancies are not great.

Figure 10

With another differentiation the edges show up clearly again and although the values have the right general sense the field still suffers from being too near the bottom face of the fitted volume.

Figure 11

The geostrophic isotachs are generally quite reasonable except for the area south-west of Portugal. Examination of subsidiary output from the computer revealed that a flaw in the logic of the background insertion routine had resulted in a badly needed background value not being inserted in this area. This failure affected all levels.

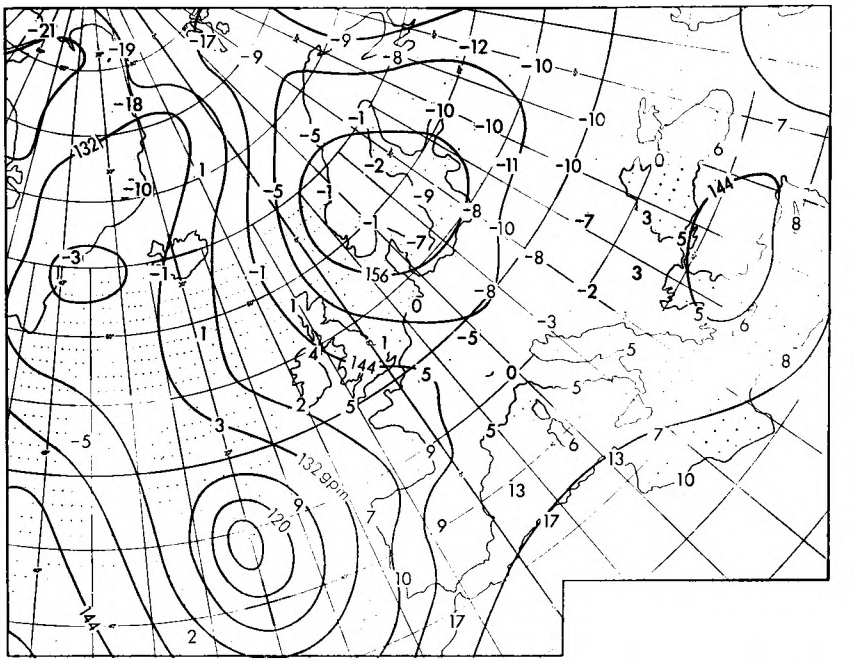

FIGURE 7. Contours at 850 mb for 00 GMT, 14 November 1968, hand-drawn in the Central Forecasting Office.
Contours are at intervals of 6 geopotential decametres.
Temperatures in degrees Celsius are shown for selected locations.

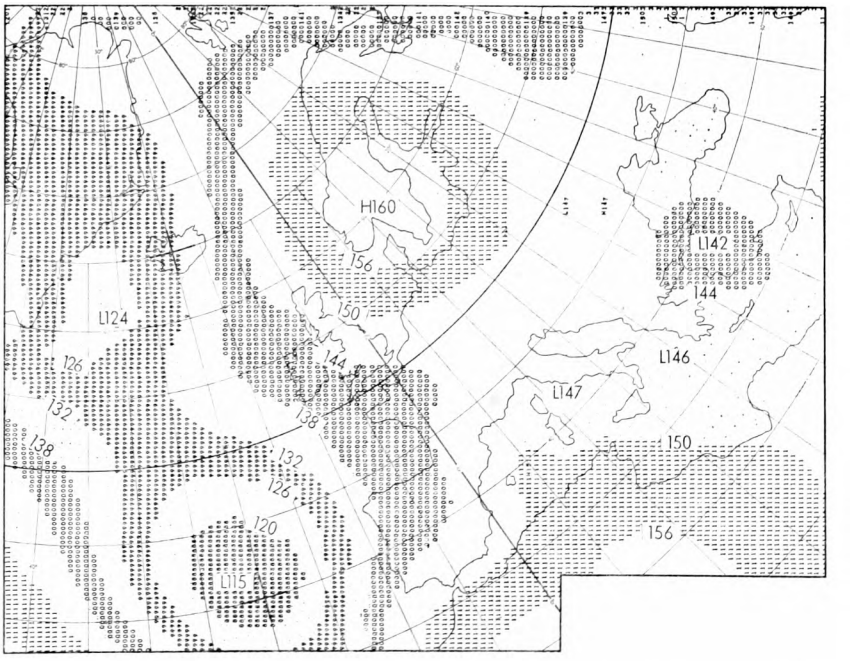

FIGURE 8. Cross-section at 850 mb of 6th-power trivariate polynomials.
Contours are at intervals of 6 geopotential decametres.

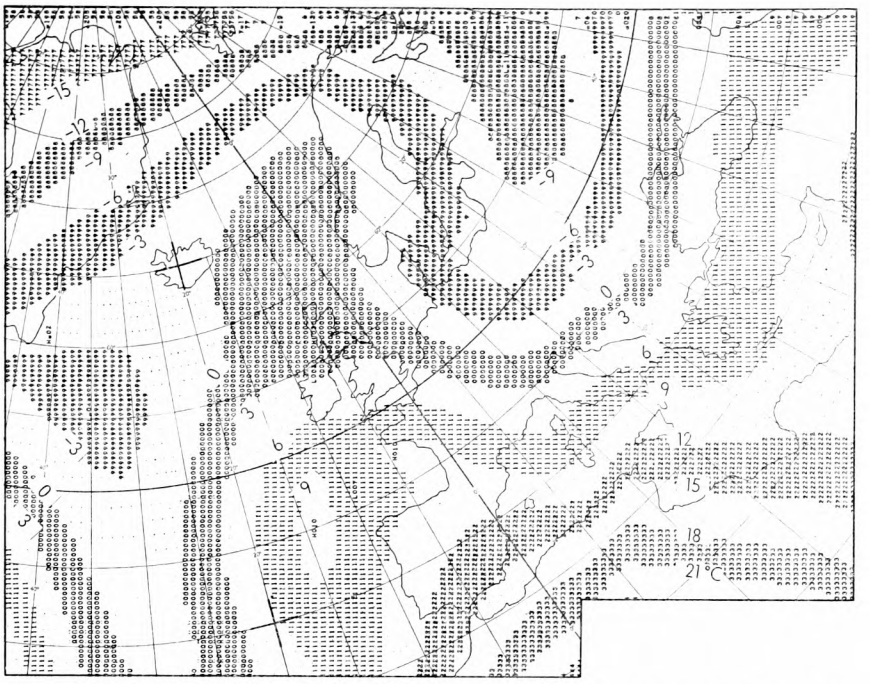

FIGURE 9. Isotherms at 850 mb obtained by differentiation of the 6th-power trivariate polynomials.
Isotherms are at intervals of 3 degC.

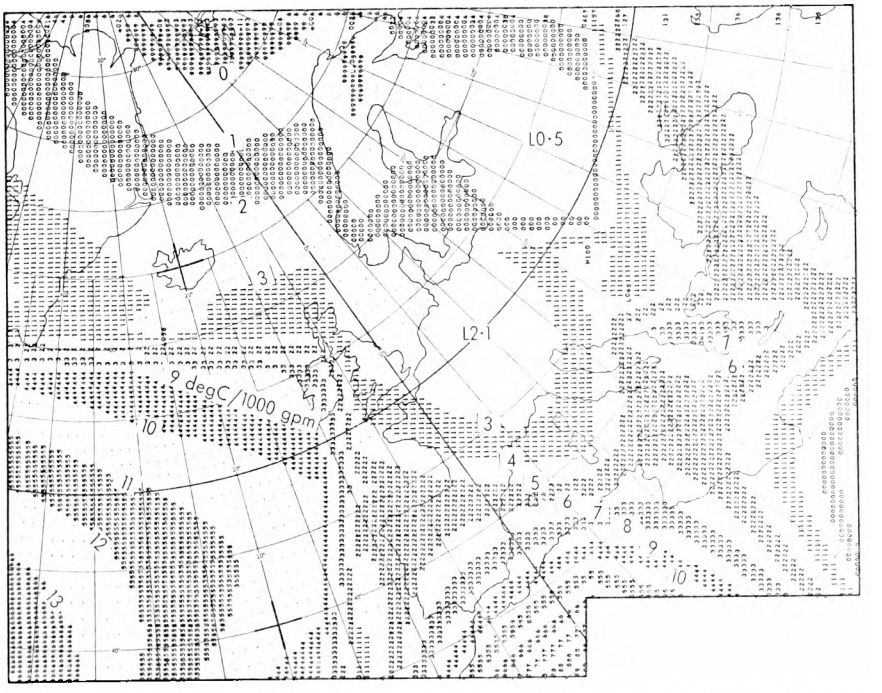

FIGURE 10. Isopleths of lapse rate at 850 mb obtained by differentiation of the 6th-power trivariate polynomials.
Isopleths are at intervals of 1 degC/1000 gpm.

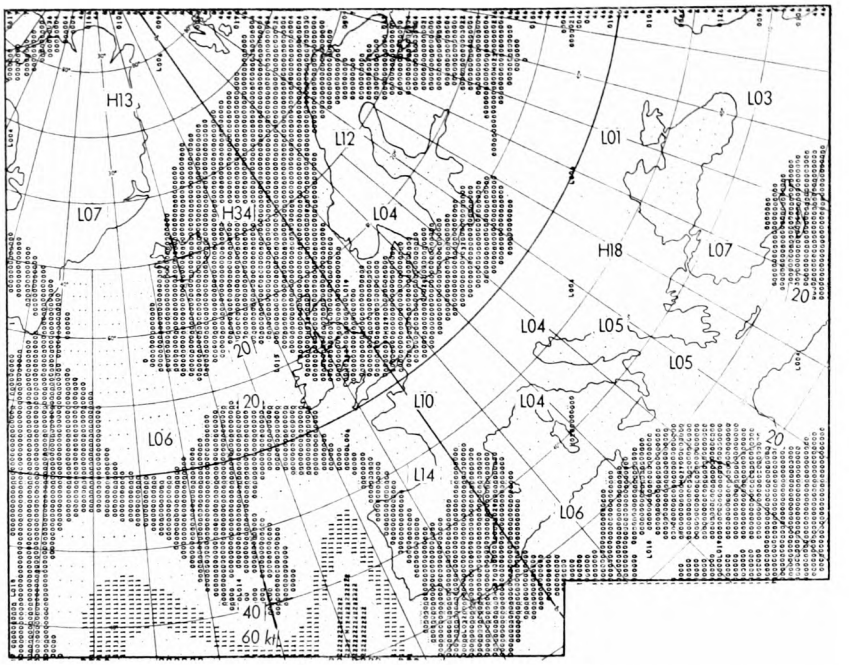

FIGURE 11. Geostrophic isotachs at 850 mb obtained by differentiation of the 6th-power trivariate polynomials.
Isotachs are at intervals of 20 kt.

THE 700-MB EVALUATIONS

Figure 13

With the exception of the situation near ocean weather station 'A' the main features are positioned and valued quite accurately. Of particular note is the fact that some minor features such as the trough near the English Channel and the kidney-shaped double trough to the west of the Black Sea are also in evidence.

Figure 14

Over wide areas of the chart the accuracy of the temperature field now surpasses what was reasonably expected from this preliminary experiment. It will be noted that even over the Atlantic most temperatures are within about 2 degC of the reported 700-mb standard-level values. One of the most serious errors appears over the English Channel region where the sixth-power fitting has been able to fit the trough in the height field but has not had enough degrees of freedom to account for the trough in the temperature field.

Figure 15

Though the lapse-rate field has become more coherent and the edges less evident within the body of the fitted volume, lack of experience of this type of output makes it difficult to comment. The case dealt with is not a particularly interesting one from the thermal point of view, the fronts shown in Figure 2 all being rather weak features in the thermal field.

Figure 16

The geostrophic isotach pattern is again reasonable, such features as the belt of light winds from the Caspian Sea to Eire, the region of 30–40-kt southerlies between Norway and Iceland, and the 30-kt north-easterlies over the southern Baltic being depicted quite well.

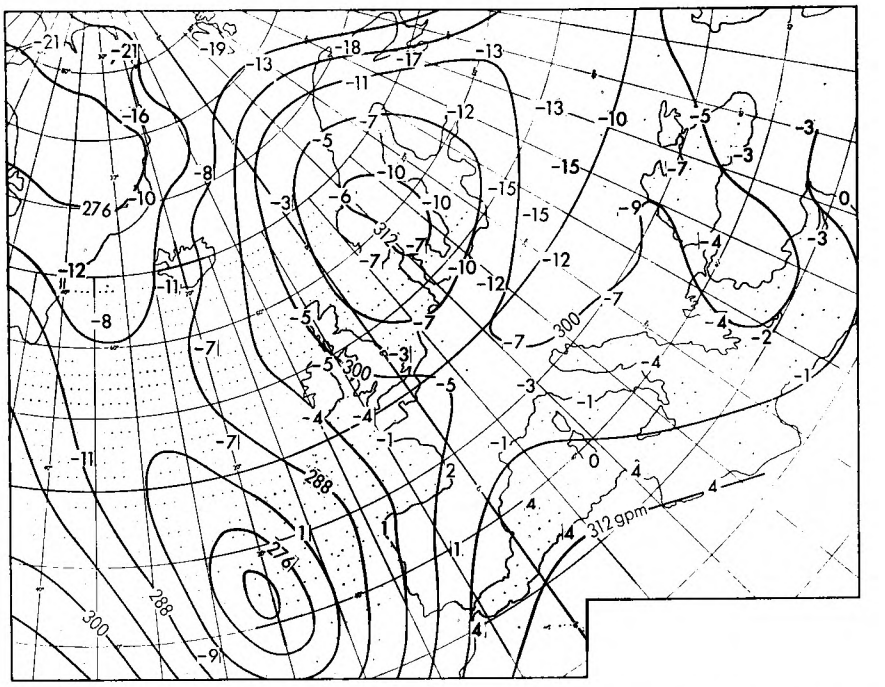

FIGURE 12. Contours at 700 mb for 00 GMT, 14 November 1968, hand-drawn in the Central Forecasting Office.
Contours are at intervals of 6 geopotential decametres.
Temperatures in degrees Celsius are shown for selected locations.

FIGURE 13. Cross-section at 700 mb of 6th-power trivariate polynomials.
Contours are at intervals of 6 geopotential decametres.

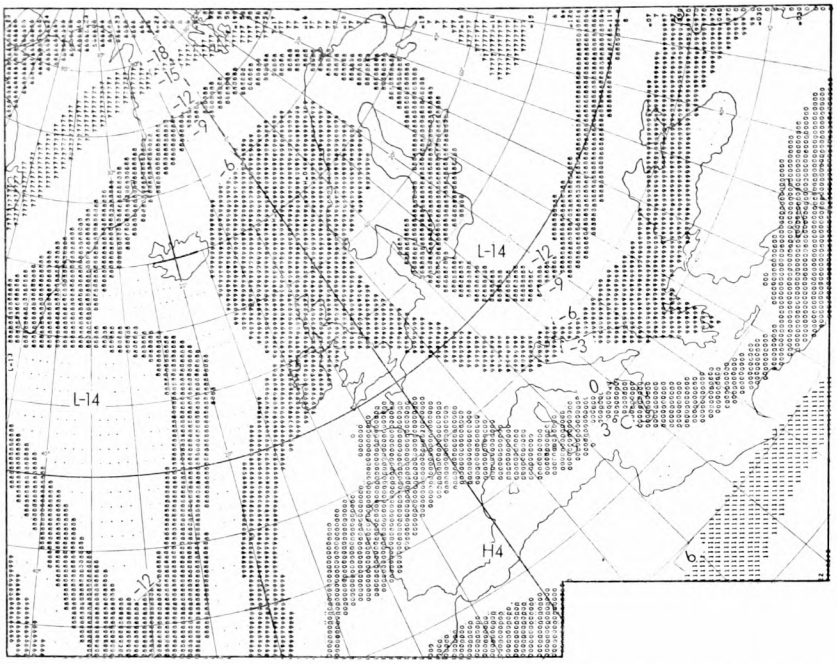

FIGURE 14. Isotherms at 700 mb obtained by differentiation of the 6th-power trivariate polynomials.
Isotherms are at intervals of 3 degC.

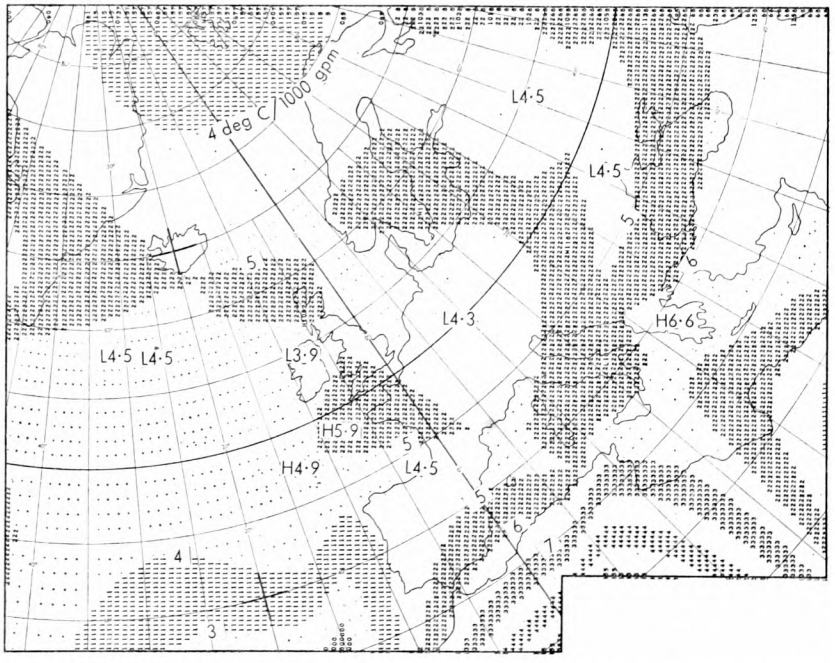

FIGURE 15. Isopleths of lapse rate at 700 mb obtained by differentiation of the 6th-power trivariate polynomials.
Isopleths are at intervals of 1 degC/1000 gpm.

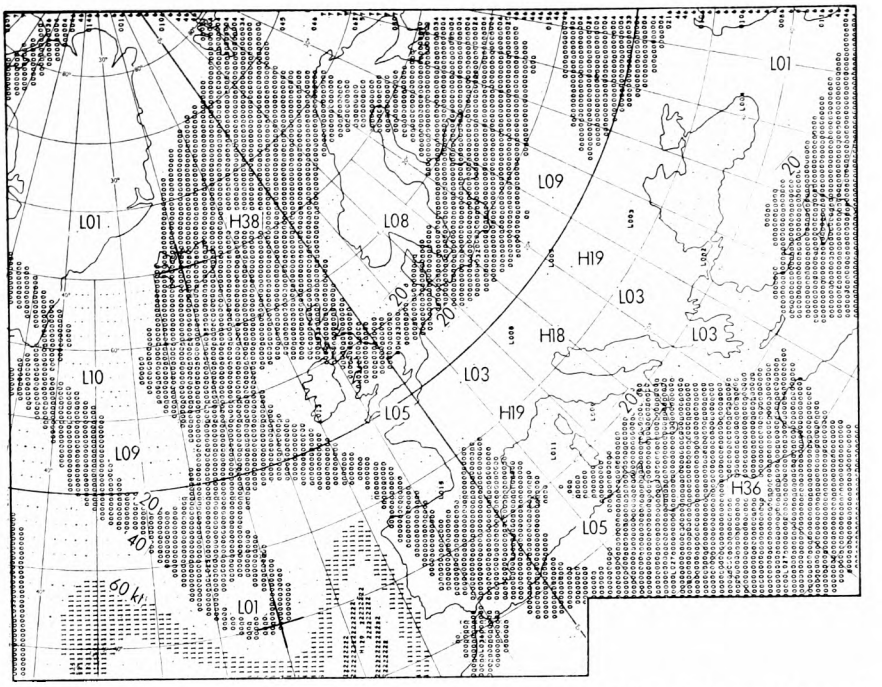

FIGURE 16. Geostrophic isotachs at 700 mb obtained by differentiation of the 6th-power trivariate polynomials.
Isotachs are at intervals of 20 kt.

THE 500-MB EVALUATIONS

Figure 18

The main features at this level are also well depicted, though it is noticeable that the gradient over the southern Baltic is not tight enough, and the trough over Russia is somewhat too smooth.

Figure 19

Considering the various shortcomings of design and data-handling accepted in this trial, the accuracy of some of the temperature fields obtained by differentiation has been an agreeable surprise, and this aspect is well illustrated by this chart, except for parts of the Atlantic, where discrepancies are accounted for by lack of data.

Figure 20

The remarks made about the 700-mb lapse rate field also apply at this level, but it is worth noting that the area of high lapse-rate over western Turkey coincides with an area of thunderstorms on the CFO surface chart.

Figure 21

Whilst substantially correct the geostrophic isotachs bring out clearly the underfitting of the Baltic north-easterlies, though some allowance has to be made for curvature.

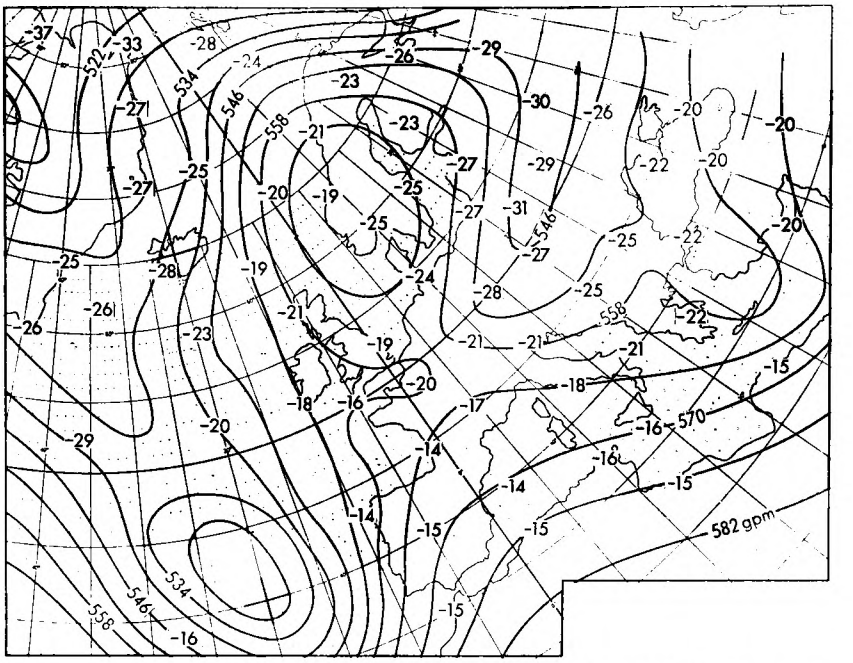

FIGURE 17. Contours at 500 mb for 00 GMT, 14 November 1968, hand-drawn in the Central Forecasting Office.
Contours are at intervals of 6 geopotential decametres.
Temperatures in degrees Celsius are shown for selected locations.

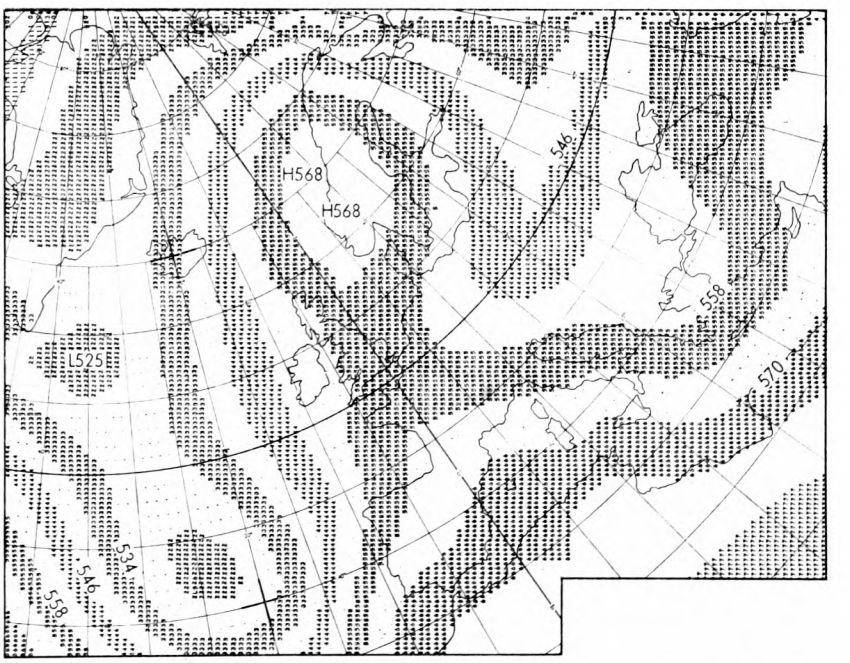

FIGURE 18. Cross-section at 500 mb of 6th-power trivariate polynomials.
Contours are at intervals of 6 geopotential decametres.

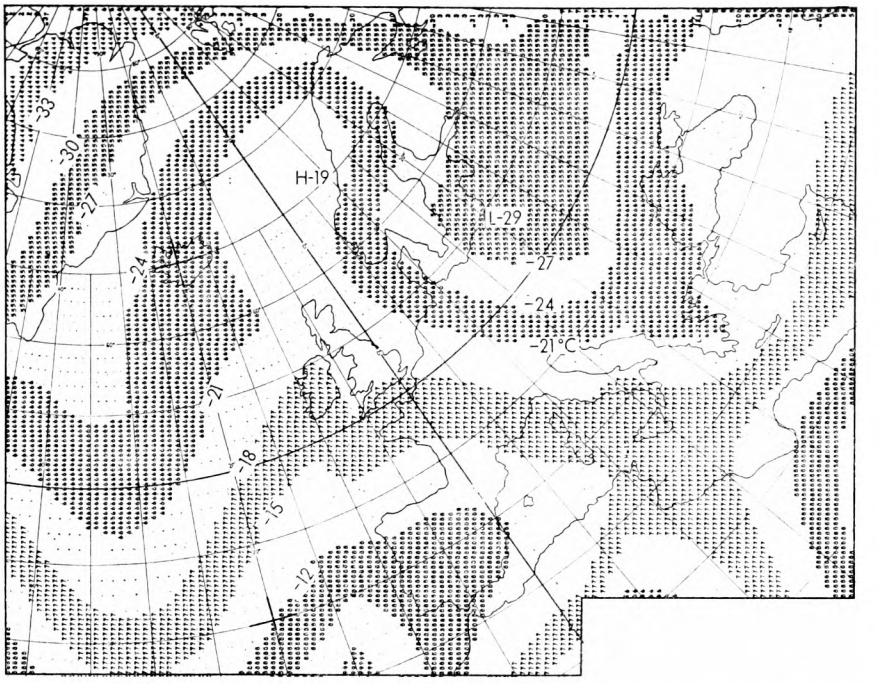

FIGURE 19. Isotherms at 500 mb obtained by differentiation of the 6th-power trivariate polynomials.
Isotherms are at intervals of 3 degC.

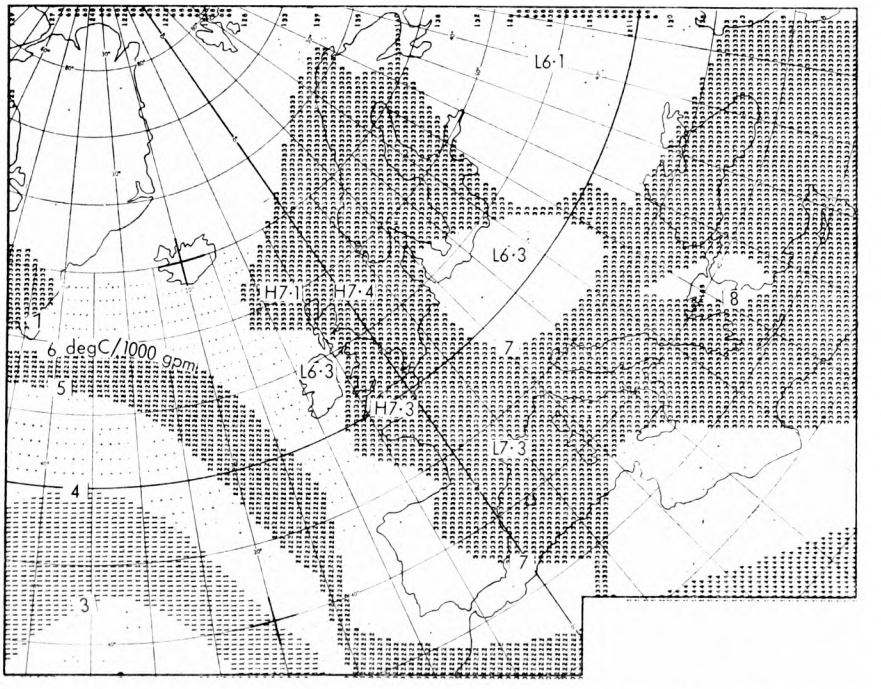

FIGURE 20. Isopleths of lapse rate at 500 mb obtained by differentiation of the 6th-power trivariate polynomials.
Isopleths are at intervals of 1 degC/1000 gpm.

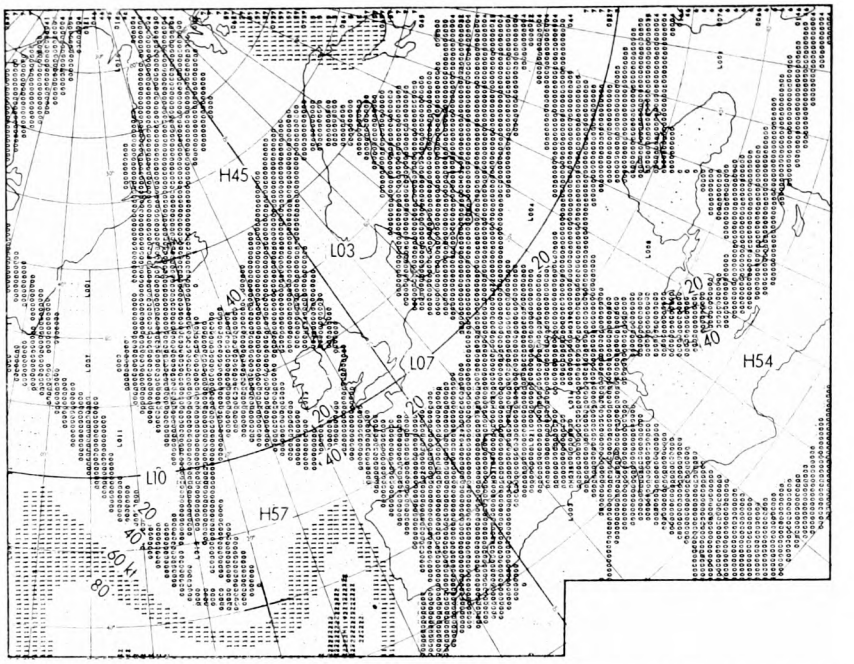

FIGURE 21. Geostrophic isotachs at 500 mb obtained by differentiation of the 6th-power trivariate polynomials.
Isotachs are at intervals of 20 kt.

THE 200-MB EVALUATIONS

Figure 23

The analysed pattern is still substantially correct, even though at this level the influence of random and systematic errors in the data is considerable. Of considerable importance is the fact that for the low near the Azores the fitting process has successfully followed the transition from a fairly intense closed circulation at low levels to an open trough at this level.

Figure 24

The accuracy of the temperature field is beginning to fall off now as the upper limit of the fitted volume is approached. Contributory reasons are the thinning out of the observations available and a change in the definition of the ICAO standard atmosphere near this level, leading to a discontinuity in vertical derivatives of the *D*-values.

Figure 25

The lapse-rate field begins to show the edges of the separate areas markedly again. The quality of the field has degenerated as compared with the 700-mb and 500-mb levels. It is noteworthy however that the region of high lapse rate over Norway is situated in the region where high tropospheric air extends to this level.

Figure 26

The sixth-power fitting has not had enough degrees of freedom to fit all the strong winds accurately, a notable deficiency being in the vicinity of ocean weather station 'C', where it is known that a poor background field contributed to the fitting problem.

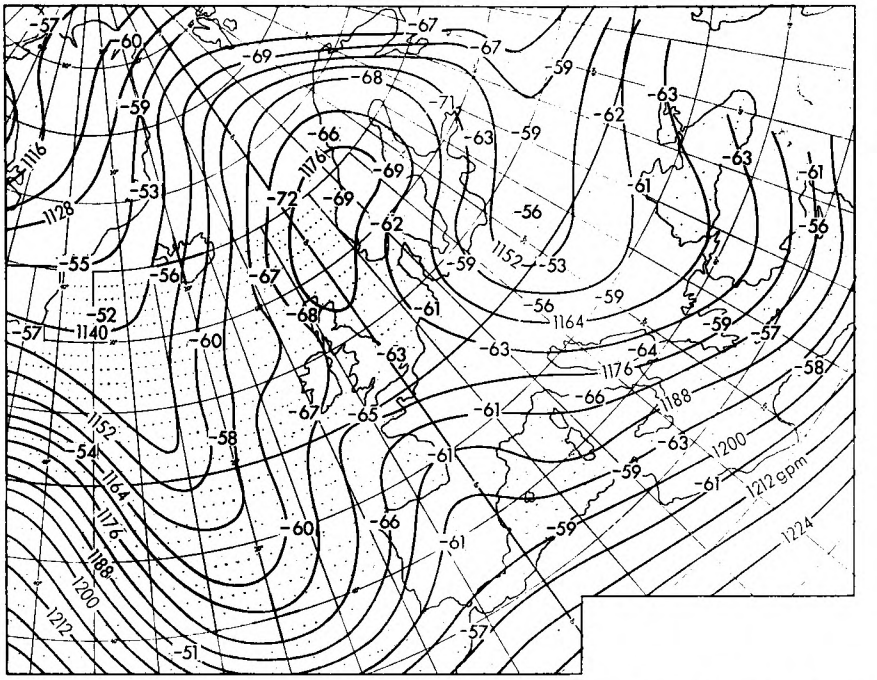

FIGURE 22. Contours at 200 mb for 00 GMT, 14 November, 1968 hand-drawn in the Central Forecasting Office.
Contours are at intervals of 6 geopotential decametres.
Temperatures in degrees Celsius are shown for selected locations.

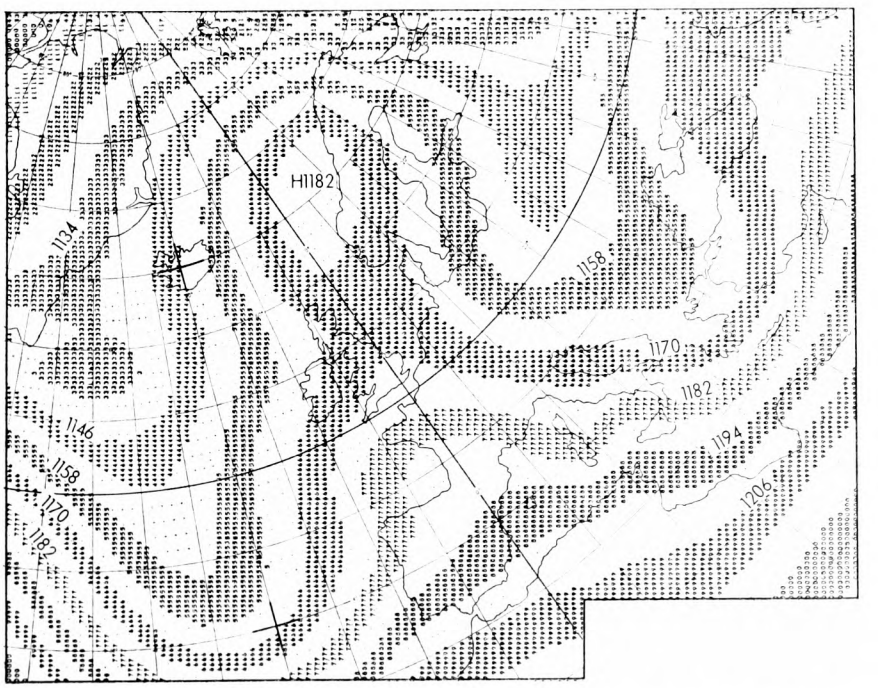

FIGURE 23. Cross-section at 200 mb of 6th-power trivariate polynomials.
Contours are at intervals of 6 geopotential decametres.

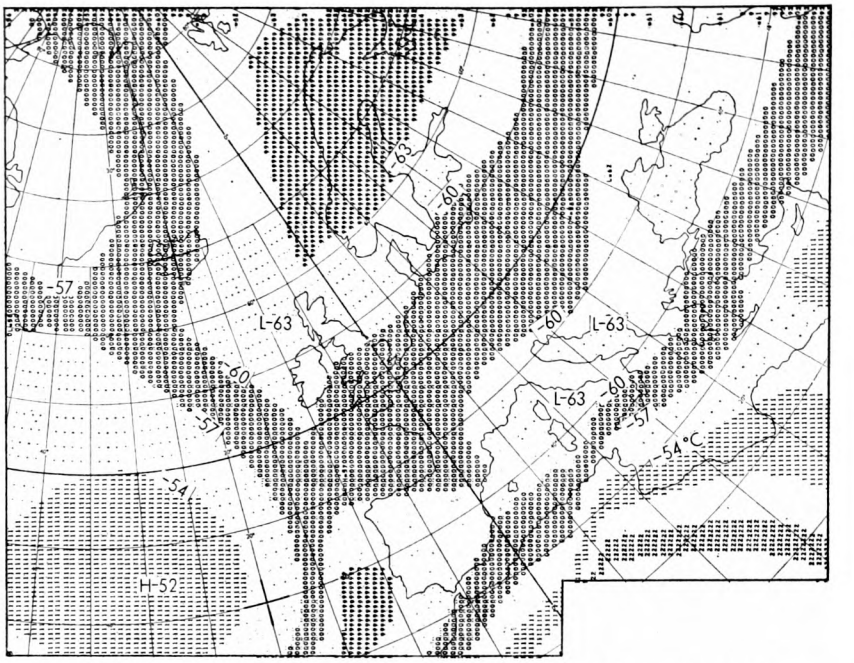

FIGURE 24. Isotherms at 200 mb obtained by differentiation of the 6th-power trivariate polynomials.
Isotherms are at intervals of 3 degC.

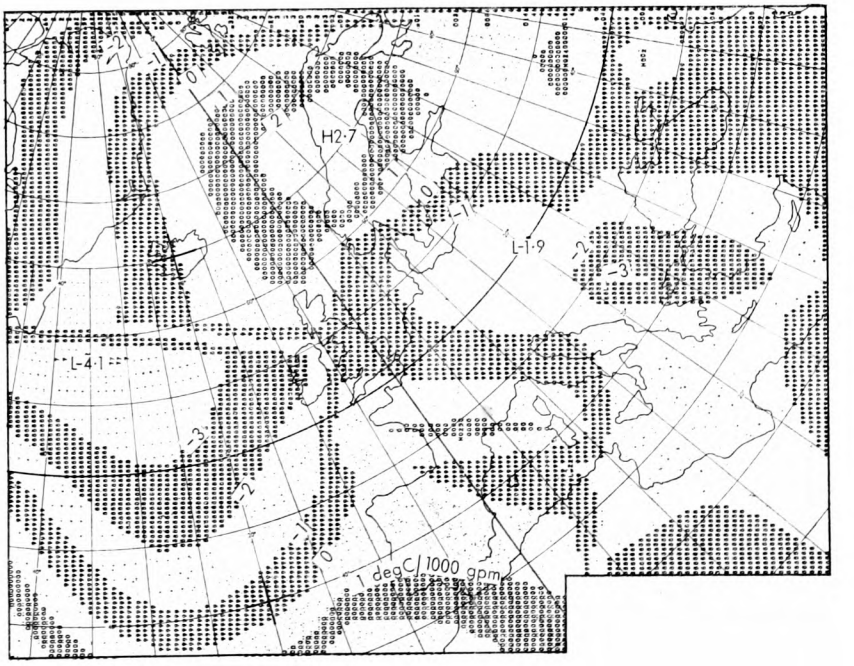

FIGURE 25. Isopleths of lapse rate at 200 mb obtained by differentiation of the 6th-power trivariate polynomials.
Isopleths are at intervals of 1 degC/1000 gpm.

FIGURE 26. Geostrophic isotachs at 200 mb obtained by differentiation of the 6th-power trivariate polynomials.
Isotachs are at intervals of 20 kt.

THE 100-MB EVALUATIONS

Figure 28

Whilst the broad features of the contour pattern are there, the disrupting influence of the random and systematic errors at this level is plainly seen.

The temperature and lapse-rate fields for this level were too incoherent to be worth reproducing, the disadvantage associated with being on a face of the fitted volume having been exacerbated by the errors in the data.

Figure 29

The geostrophic isotachs are reasonable except to the extent that the height contours are themselves wrong. It is interesting to note that the incoherence of the vertically differentiated fields does not affect this field obtained by horizontal differentiation.

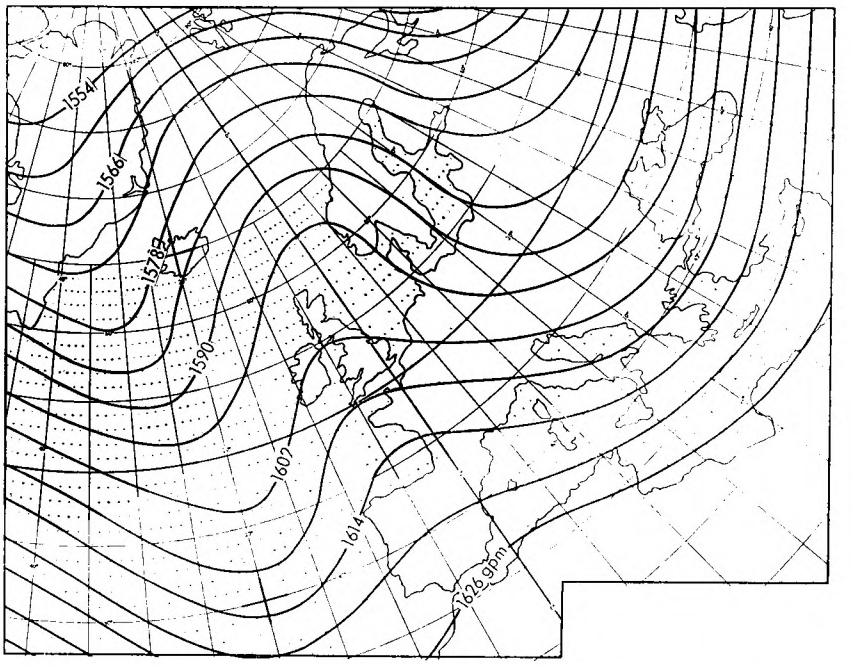

FIGURE 27. Contours at 100 mb for 00 GMT, 14 November 1968, hand-drawn in the Central Forecasting Office.
Contours are at intervals of 6 geopotential decametres.

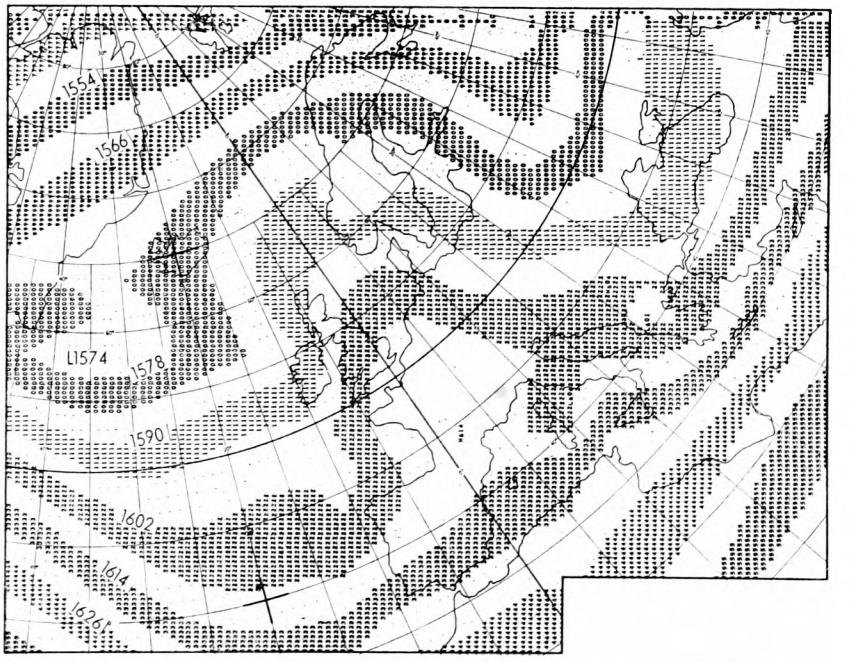

FIGURE 28. Cross-section at 100 mb of 6th-power trivariate polynomials.
Contours are at intervals of 6 geopotential decametres.

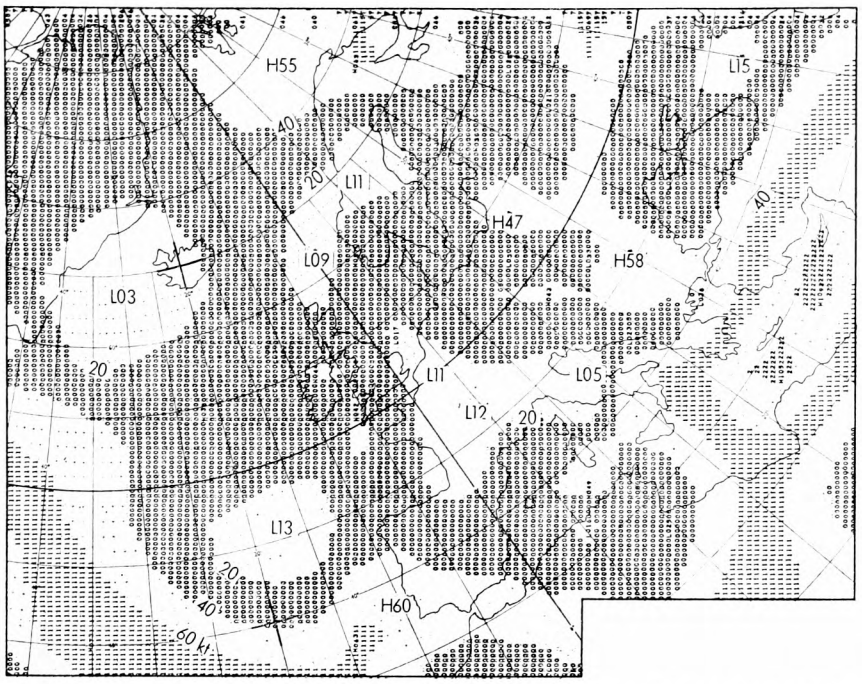

FIGURE 29. Geostrophic isotachs at 100 mb obtained by differentiation of the 6th-power trivariate polynomials.
Isotachs are at intervals of 20 kt.

THE MSL PRESSURE CHART

Figure 30

Comparing this chart with Figure 31, it is seen that with the exception of the area near ocean weather station 'A' the surface analysis produced is of about the same standard as one produced by the full operational routine. This is a noteworthy feature of the experiment considering that only the surface reports of the significant-level messages were used and none of the great mass of surface observations which were available. The result is thought to illustrate some comments by Smagorinsky[9] on the greater information content of observations distributed throughout the space (or space/time) under analysis, as compared with the information content of observations concentrated at some particular level or time. The result also appears to support his argument for the existence of a so far unutilized degree of redundancy amongst the physical variables.

FIGURE 30. MSL surface pressure chart obtained from the 6th-power trivariate polynomials.
Isobars are at intervals of 4 mb.

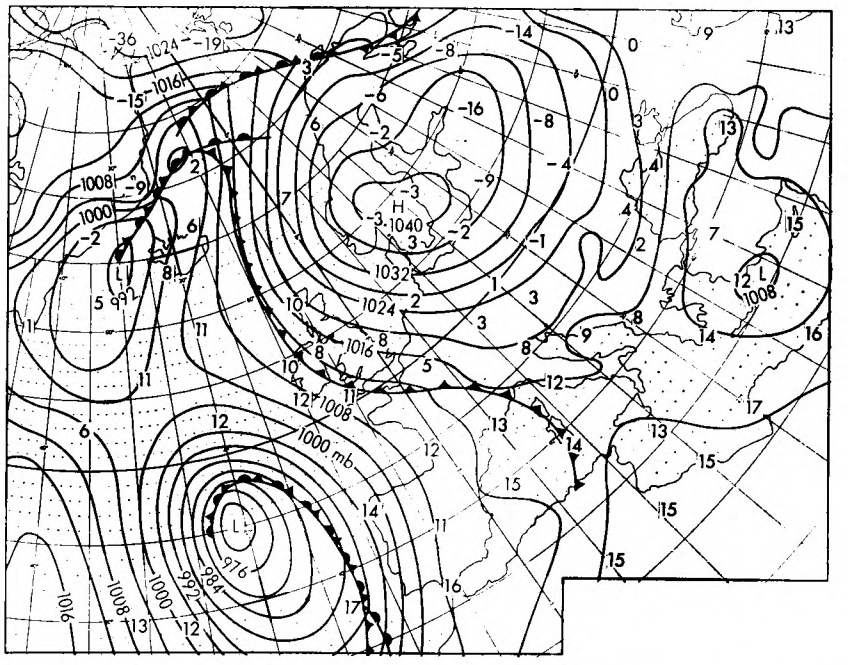

FIGURE 31. MSL surface pressure chart for 00 GMT, 14 November 1968, hand-drawn in the Central Forecasting Office. Isobars are at intervals of 4 mb. Temperatures in degrees Celsius are shown for selected locations.

COMMENTS

It is considered that these preliminary results point to the feasibility of this type of analysis, though it will be necessary to conduct further trials with a more comprehensive scheme as soon as the necessary computer capacity is available. In particular the limits of the technique need exploring to determine what volume of raw data can be fitted by one function. The size of the volume which can be fitted by one function is likely to be limited by the ultimate re-emergence of the round-off error problem in the Gram-Schmidt process, but at present the stage at which this will occur cannot be determined. It may be noted that when the round-off problem does reappear it should be possible to prolong the process further by a second application of the orthonormalizing routine. Thus if a fitting to a large number of observations to a very high power were being attempted the result of the Gram-Schmidt process might be a somewhat contaminated set of orthogonal vectors, but if the Gram-Schmidt process were then applied to this set the final result should be a much more strictly orthogonal set. Other questions to be resolved by experiment are such matters as whether or not it would be better to fit the atmosphere in two layers, troposphere and stratosphere, rather than in one. It seems desirable too that any weighting scheme introduced should take account of the way in which the accuracy of soundings falls off with height. There is also the question of the relative degree of fitting in the different variables. Whilst it seems natural that x and y should be of the same power, if very large volumes are fitted it may be necessary to modify the process to limit the power of the vertical variable.

The amount and variety of output readily obtained from a three-dimensional fitting has been demonstrated. There is a similar flexibility available in the arrangement and ordering of the fitting computations themselves. When an orthonormalizing code is used the process of representing data by a polynomial falls naturally into three stages:

Stage of fitting	Relative time		
	2 dimensions	3 dimensions	4 dimensions
1. Orthonormalization	50	500	5000
2. Evaluation of coefficients	1	10	100
3. Evaluation of polynomial	1	3	6

The figures quoted under 'relative time' in the above table are rough values, since the exact values depend upon precisely what is being done, i.e. number of observations, power of fitting, etc. An important point is that Stage 1, which is by far the most time-consuming, is concerned only with the base functions themselves. The observed values of the dependent variable do not come into the process until Stage 2.

If the computing capacity available in the future is more than adequate for the fitting problem being tackled so that there is no operational real-time difficulty then all three stages can be gone through, the appropriate orthonormal base vectors being computed each time. In this way the maximum versatility and power of the method can be brought to bear.

If the computing capacity is such that a moderate real-time difficulty exists then it should be possible to remove a substantial proportion of the Stage 1 time from the real-time domain by taking advantage of the fact that this stage is concerned only with data positions. This can be done by computing the orthonormal base functions for some given data set and retaining them for use with later data sets. Of course for any given later data set the evaluated base vectors will not be quite orthonormal since the pattern of the observations will not be quite the same as that for which the base functions were computed. However, this merely

means that the process generates a diagonally dominant matrix in the normal equations instead of a completely diagonal one as in the strictly orthogonal case. The diagonally dominant matrix is positive definite and so the system should be rapidly solved by an appropriate iterative technique. It is intended to present evidence on the application of this technique in a subsequent paper.

If the computing capacity is such that there is considerable difficulty in tackling the problem in real time by either of the above schemes, then it can be arranged that all of Stage 1 is removed from real time, and is replaced in real time by one or two trivial routines. This possibility arises from the fact that the grid-point values of the 12-hour forecasts from, say, a 10-level model, together with the observations from the fixed stations will provide a large array of data values from a fixed 3- or 4-dimensional array of base positions. The orthonormal functions and vectors for this array can be calculated once and for all and used for all cases, leaving only the relatively quick Stages 2 and 3 to be done. Stations which failed to report could have an interpolated value supplied from the background data. Observations available at positions not taken into account in computing the orthonormal vectors could be used to adjust the values at the nearest base points by means of some distance-weighted influence function. Aircraft reports could be similarly dealt with after first having a D-value allocated to them by interpolation from a background field.

The speed of analysis attainable by this method using precomputed vectors would be very high. For example on a computer 100 times as fast as KDF 9 it would take only approximately 16 seconds of central processor time to perform Stages 2 and 3 for a 20th-power $f(x, y, p, t)$ fit evaluated over a hemispherical grid of 2800 points for some one particular time and level. For any other level and time required only approximately 8 seconds would be needed as only Stage 3 would have to be performed.

ACKNOWLEDGEMENT

We are indebted to Mr. J. H. Cadwell of the Mathematics Department, Royal Aircraft Establishment, Farnborough, for the Gram-Schmidt routine used in this experiment.

BIBLIOGRAPHY

1. DIXON, R.; Orthogonal polynomials as a basis for objective analysis. *Scient. Pap. met. Off., London*, No. 30, 1969.
2. RICE, J. R.; Experiments on Gram-Schmidt orthogonalization. *Maths Comput., Providence, R.I.*, 20, 1966, pp. 325–328.
3. JORDAN, T. L.; Experiments on error growth associated with some linear least-squares procedures. *Maths Comput., Providence, R.I.*, **22**, 1968, pp. 579–588.
4. CADWELL, J. H. and WILLIAMS, D. E.; Some orthogonal methods of curve and surface fitting. *Comput. Jnl, London*, **4**, 1961, pp. 260–264.
5. TODD, J.; Survey of numerical analysis. New York, McGraw-Hill, 1962.
6. GANDIN, L. S.; Objective analysis of meteorological fields. (Translated from the Russian by the Israel Program for Scientific Translations, Jerusalem.) London, Oldbourne Press, 1965.
7. KRUGER, H. B.; General and special approaches to the problem of objective analysis of meteorological variables. *Q. Jnl R. met. Soc., London*, **95**, 1969, pp. 21–39.
8. FOUGERE, P. F.; Mutually consistent magnetic charts based on orthogonal functions. *Jnl geophys. Res., Baltimore*, **69**, 1964, pp. 2641–2650.
9. SMAGORINSKY, J.; Problems and promises of deterministic extended range forecasting. *Bull. Amer. met. Soc., Lancaster, Pa.*, **50**, 1969, pp. 286–311.

Printed in Scotland for Her Majesty's Stationery Office by David J. Clark Ltd.
(O.N.PS502551) Dd.501099 K8 10/70 Gp.521

© *Crown copyright 1970*

Published by
HER MAJESTY'S STATIONERY OFFICE

To be purchased from
49 High Holborn, London WC1V 6HB
13a Castle Street, Edinburgh EH2 3AR
109 St Mary Street, Cardiff CF1 1JW
Brazennose Street, Manchester M60 8AS
50 Fairfax Street, Bristol BS1 3DE
258 Broad Street, Birmingham 1
7 Linenhall Street, Belfast BT2 8AY
or through booksellers

SBN 11 400173 1